

ISSN 0389-4010
UDC 519.213: 519.245
624.078.44: 629.7.015.4
629.7.017: 629.7.023

航空宇宙技術研究所報告

TECHNICAL REPORT OF NATIONAL AEROSPACE LABORATORY

TR-1283T

A Residual Strength Analysis of a Cracked Stiffened Panel
with Stochastic Factors in Fastener Flexibility

Hirokazu SHOJI

1996年2月

航空宇宙技術研究所
NATIONAL AEROSPACE LABORATORY

目 次

概要	3
1. Introduction	4
2. Description of Formulation	4
2.1 Description of an Analytical Model	4
2.2 The Outline of DCM	4
2.2.1 Sheet Displacements	4
2.2.2 Outer Intact Stiffener Displacements	7
2.2.3 Center Broken Stiffener Displacements	7
2.2.4 Compatibility of Displacements	7
2.2.5 Sheet Displacements	7
2.2.6 Crack-tip Stress Intensity Factor	8
2.3 Description of a Method of Considering Stochastic Factors	8
3. A Study of Differences in Distribution Models of Fastener Flexibility ¹⁹⁾	9
3.1 Description of Models	9
3.2 Details of the Panel Model	9
3.3 Results and Discussion	9
4. Results and Discussion of Residual Strength Analysis ²¹⁾	10
5. Conclusions	11
Acknowledgements	12
Reference	12

A Residual Strength Analysis of a Cracked Stiffened Panel with Stochastic Factors in Fastener Flexibility*

Hirokazu SHOJI*¹

ABSTRACT

In this report, a residual strength analysis of a cracked stiffened panel was conducted on the basis of the displacement compatibility method, which is generally used as a handy tool. Stochastic factors in fastener flexibility are considered in the analysis by Monte Carlo simulation. The report outlines the displacement compatibility method, a method of taking in stochastic factors into account, some results of differences in stochastic distribution models in fastener flexibility, and some results of the analysis. The author shows that the stochastic flexibility coefficients in rivet fastening affect the residual strength estimation of a cracked stiffened panel considerably.

Keywords: Damage Tolerance Design, Residual Strength, Crack, Stiffened Panel, Stochastic Factor, Fastener, Monte Carlo Simulation

概 要

亀裂を有する補強パネルに対して、その簡便さのために広く利用されている変位適合法を基に残留強度解析を行った。解析では、モンテカルロシミュレーションによりファスナー結合の柔軟性の不確実要因が考慮された。この報告書では、変位適合法の概要、不確実要因の取り込み方、ファスナー結合の柔軟性の不確実な分布モデルの違いによる結果、そして残留強度解析の結果を示す。ファスナー結合の不確実な柔軟係数が亀裂を有する補強パネルの残留強度評価に影響を及ぼすことが示された。

1. Introduction

The design of a transport category airframe requires the evaluation of damage tolerance in compliance with present airworthiness standards, such as FAR25.571¹⁾. Before the damage tolerance of an airframe can be certified, we have to show that any damage initiated by fatigue, accident, manufacturing defects or corrosion will be detected before catastrophic failure^{2),3)}. Thus, an engineering evaluation considering crack propagation rates and residual strength limits is made by the manufacturer, and inspections are carried out by the operator²⁾. The evaluation must be made with tests and analyses, but the tests are expensive and labor-intensive. Therefore, if we can substitute some analyses for some tests, we can save time and cost.

In general, deterministic values, which are usually mean values, of material properties and geometry are used in analyses of airframe structures. In practice, however, real airframe structures have stochastic factors, such as degradation of material properties owing to corrosion, initiated crack locations and sizes, fastener flexibility, etc., so that a lot of tests are required for the evaluation. Thus, we analyze them with uncertain values and evaluate the results, although we have to study methods of analysis and evaluation. If the analyses show good results in simulating real airframe structures, it may be possible to substitute an analysis for a test. As the first step of accomplishing this substitution, a residual strength analysis on a stiffened panel, which is broadly used in airframe structures, with considering stochastic factors in fastener flexibility is carried out.

* received 25 December 1995

*¹ Airframe Division

When a residual strength analysis was performed for a cracked stiffened panel, the finite element method (FEM) or the displacement compatibility method (DCM) is usually chosen. In this paper, the DCM is chosen because it is a handy tool owing to its small matrix size, which is due to its analytical formulation using fracture mechanics methodology. It was originally proposed by Poe^{4,5}, and Swift^{6,7} made it practical by including fastener flexibility and stiffener bending. Sasaki et al.^{8,9} made a program which can calculate with various conditions by expanding Poe's methods. Nishimura^{10,12} expanded its applicability to include a multiple-cracked stiffened panel. Yeh¹³ applied it to a stiffened orthotropic sheet. Now Swift's formulation is used with ignoring stiffener bending and considering stochastic factors in fastener flexibility because it is elegant and easy to consider them.

In this paper, an outline of Swift's formulation is shown. A method of considering stochastic factors in fastener flexibility by a Monte Carlo simulation method, and a study of differences in distribution models of stochastic factors are proposed. The results of residual strength analyses of a cracked stiffened panel are reported. The author also shows that stochastic factors in fastener flexibility take effects in an estimation of residual strength of a cracked stiffened panel considerably.

2. Description of Formulation

2.1 Description of an Analytical Model

In damage tolerance design, a two-bay skin crack with a broken center stiffener at limit load is considered and is certified to survive. This large damage capability is necessary to be simulated in case a fast fracture occurs from a shorter crack which might have been overlooked on regular inspections, and discrete source or foreign object damage as in the case of an engine disintegration². Now, we consider a two-bay panel with a broken center stiffener (Fig. 1).

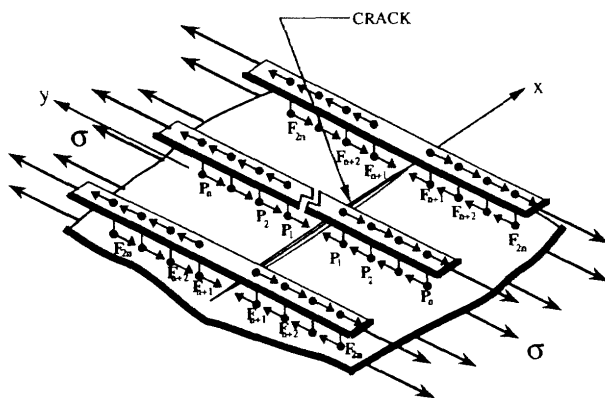


Fig. 1. Schematic diagram of an analysis model for a cracked stiffened panel

In Fig. 1, the analysis model is a cracked panel with fastened strip stiffeners, which are used for simplicity, subjected to the uniaxial remote stress σ . The forces are transferred into the stiffeners from the sheet through the fastener system and redistributed into the intact stiffeners as the crack propagates. As required by equilibrium, the fastener forces act in opposite directions on the sheet and stiffeners. It is assumed that the center of the crack is located symmetrically underneath the mid-line of the broken center stiffener and the crack is perpendicular to the loading direction and extends equally on both sides of the center stiffener; therefore, the fastener forces act symmetrically with respect to the crack. The coordinate system is as follows: the x-axis is parallel to the direction of propagation of the crack, the y-axis is parallel to the direction of loading or the stiffeners, and the origin is the center of the crack. We consider the area of three stiffeners only because additional outboard stiffeners have little effect on a crack within two bays⁶.

We solve the problem by the compatibility of the displacement between the sheet and the stiffeners; that is, we make an equilibrium equation relating to the compatibility with fastener forces as unknown quantities. We acquire the results of a residual strength analysis of the cracked stiffened panel from the crack tip intensity factor calculated by unknown fastener forces. Because the crack and the structure are symmetrical, we may consider only the part of two stringers, the center stiffener and the one outer stiffener, above the x-axis. In Fig. 1, P_i s are unknown fastener forces on the broken center stiffener and F_i s are forces on the intact outer stiffener. We analyze the problem with considering fastener flexibility, which is expressed as linear coefficients of fastener forces, as stochastic factors.

2.2 The Outline of the DCM

As mentioned above, we use Swift's formulation of the DCM. An outline of this formulation is contained in references 6 and 7.

2.2.1 Sheet Displacements

For this analytical model the cracked sheet displacements are obtained by superposition of the four cases shown in Fig. 2. Sheet displacements resulting from the four cases are defined as follows:

v_1 ; displacement anywhere in the cracked sheet caused by the applied gross stress,

v_2 ; displacement in the uncracked sheet resulting from the outer intact stiffener fastener loads,

v_3 ; displacement in the uncracked sheet resulting from the center broken stiffener fastener loads,

and

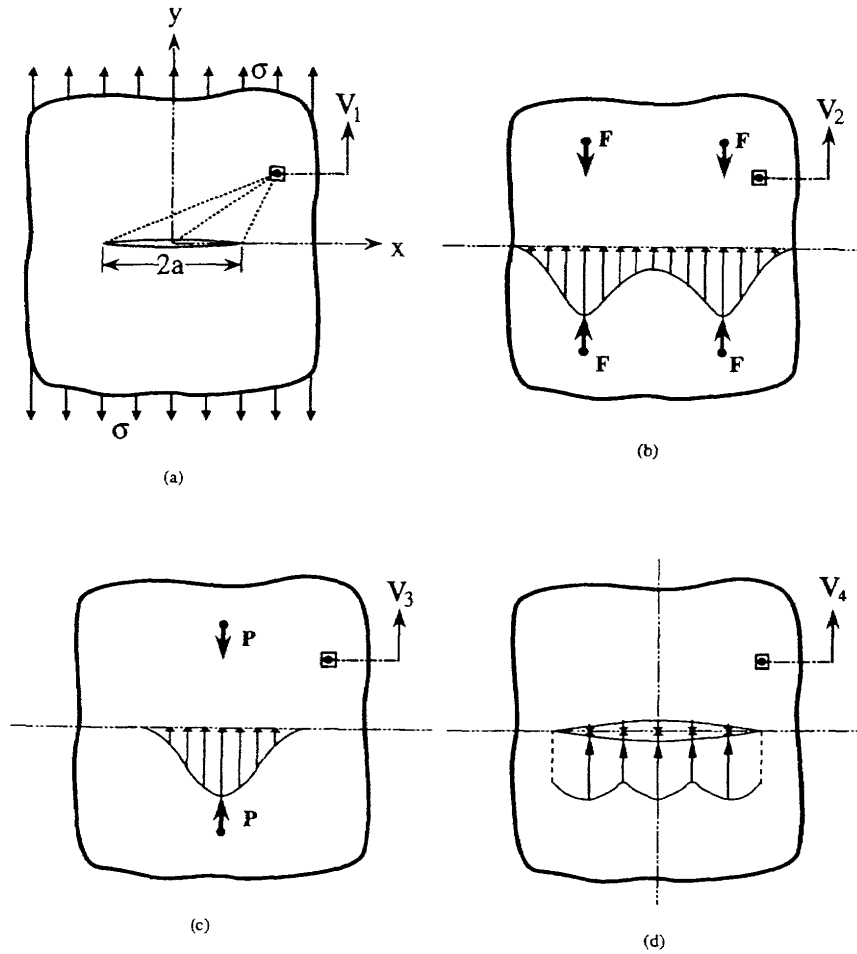


Fig. 2. Displacements that are superimposed to determine total sheet displacement

v_4 ; displacement in the cracked sheet resulting from stress which is applied to the crack face to be equal and opposite to the stresses caused by fastener loads.

For plane stress, the y-component of the sheet displacement is given by Westergaard's¹⁴⁾ complex stress function approach as follows

$$v = [2\text{Im } \bar{Z} - (1 + \nu) y \text{Re } Z] / E \quad (1)$$

For an infinite, biaxially loaded cracked sheet, the following Westergaard's¹⁴⁾ complex stress function Z that would satisfy the equilibrium and compatibility for a two-dimensional elastic problem and the boundary conditions for an infinite panel

$$Z = \sigma z / \sqrt{z^2 - a^2} = \sigma z (z^2 - a^2)^{-1/2} \quad (2)$$

where $z = x + iy$, \bar{Z} is the first integral of Z , Im and Re are the imaginary and real parts of Z , ν and E are Poisson's ratio and Young's modulus of the sheet, respectively, and a is a half crack length.

The displacement v_1 is obtained by substituting Eq. (2) into Eq.

(1) and applying a compressive stress in the x-direction to cancel out the x-component of tension stress. Thus, v_1 is given by the following equation for displacement in a uniaxially loaded cracked sheet,

$$v_1 = \sigma \left\{ 2\sqrt{r_1 r_2} \sin\left(\frac{\theta_1 + \theta_2}{2}\right) - \frac{(1 + \nu)yr}{\sqrt{r_1 r_2}} \left[\cos\left(\theta - \frac{\theta_1 + \theta_2}{2}\right) \right] + \nu y \right\} / E \quad (3)$$

where unknown nomenclatures are defined in Fig. 2 (a).

The displacement v_2 is obtained from the work of Love¹⁵⁾. The stress distribution anywhere in an infinite plate resulting from a concentrated force F can be determined as follows

$$\sigma_y = [Fy(1 + \nu) / 4\pi t (x^2 + y^2)] \{ [(3 + \nu) / (1 + \nu)] - [2x^2 / (x^2 + y^2)] \} \quad (4)$$

where t is the thickness of the sheet. The displacement v_F resulting from force F is given by

$$v_F = \left[\frac{F(1 + \nu)}{4\pi t E} \right] \left\{ \frac{3 - \nu}{2} \log(x^2 + y^2) + \frac{(1 + \nu)x^2}{x^2 + y^2} \right\} + C \quad (5)$$

where C is a constant of integration. However, this equation contains a singularity at the load center. Thus, we avoid the sin-

gularity by assuming that the concentrated force F is distributed uniformly over the fastener diameter d and integrating the effect over the fastener diameter.

Therefore, the displacement v_2 for the system of four forces like Fig. 2 (b) is given by superposition as follows

$$\begin{aligned}
 v_2(x_i, y_i, x_j, y_j) = & \frac{F_j(1+\nu)(3-\nu)}{16\pi Et} \left\{ (X_A-1) \log \left| \frac{(X_A+1)^2 + Y_A^2}{(X_A+1)^2 + Y_B^2} \right| \right. \\
 & - (X_A-1) \log \left| \frac{(X_A-1)^2 + Y_A^2}{(X_A-1)^2 + Y_B^2} \right| + (X_B-1) \log \left| \frac{(X_B+1)^2 + Y_A^2}{(X_B+1)^2 + Y_B^2} \right| \\
 & - (X_B-1) \log \left| \frac{(X_B-1)^2 + Y_A^2}{(X_B-1)^2 + Y_B^2} \right| \\
 & + 4 \left(\frac{1-\nu}{3-\nu} \right) \left[Y_A \tan^{-1} \left(\frac{2Y_A}{Y_A^2 + X_A^2 - 1} \right) + Y_A \tan^{-1} \left(\frac{2Y_A}{Y_A^2 + X_B^2 - 1} \right) \right. \\
 & \left. - Y_B \tan^{-1} \left(\frac{2Y_B}{Y_B^2 + X_A^2 - 1} \right) - Y_B \tan^{-1} \left(\frac{2Y_B}{Y_B^2 + X_B^2 - 1} \right) \right] \Bigg\} \quad (6)
 \end{aligned}$$

where

$$\begin{aligned}
 X_A &= (2/d)(x_i - x_j), \\
 X_B &= (2/d)(x_i + x_j), \\
 Y_A &= (2/d)(y_i - y_j), \text{ and} \\
 Y_B &= (2/d)(y_i + y_j).
 \end{aligned}$$

Subscripts i and j represent the point of the displacement influenced from the force and the point of the fastener force, respectively.

The displacement v_3 for the system of two forces P like Fig. 2 (c) is given in the same way as Eq.

(5) by

$$\begin{aligned}
 v_3(x_i, y_i, y_j) = & \frac{P_j(1+\nu)(3-\nu)}{16\pi Et} \left\{ \left(\frac{2r_i}{d} + 1 \right) \log \left| \frac{\left(\frac{2r_i}{d} + 1 \right)^2 + Y_A^2}{\left(\frac{2r_i}{d} + 1 \right)^2 + Y_B^2} \right| - \left(\frac{2r_j}{d} + 1 \right) \log \left| \frac{\left(\frac{2r_j}{d} + 1 \right)^2 + Y_A^2}{\left(\frac{2r_j}{d} + 1 \right)^2 + Y_B^2} \right| \right. \\
 & \left. + 4 \left(\frac{1-\nu}{3-\nu} \right) \left[Y_A \tan^{-1} \left(\frac{2Y_A}{Y_A^2 + \frac{4x_i^2}{d^2} - 1} \right) + Y_B \tan^{-1} \left(\frac{2Y_B}{Y_B^2 + \frac{4x_i^2}{d^2} - 1} \right) \right] \right\} \quad (7)
 \end{aligned}$$

The displacement v_4 is obtained by applying an equal and opposite stress distribution over the crack face to cancel out the stress caused by the fastener forces F_j s and P_j s. Furthermore, the stress distribution along the x -axis, $\sigma_y(x, 0)$, on an uncracked sheet resulting from a system of forces like Fig. 3 can be obtained from Eq. (3) by transfer of axis.

$$\sigma_y(x, 0) = - \left\{ (1+\nu) y_j / 2\pi t \right\} \left[F_j \alpha(x_j, y_j, b) + P_j \beta(y_j, b) \right] \quad (8)$$

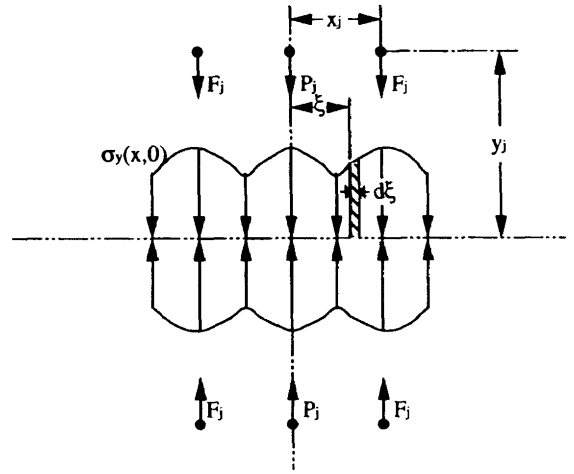


Fig. 3. Stress distribution at $y = 0$ owing to fastener loads

where

$$\begin{aligned}
 \alpha(x_j, y_j, \xi) = & \frac{3+\nu}{1+\nu} \left\{ \frac{1}{(\xi-x_j)^2 + y_j^2} + \frac{1}{(\xi+x_j)^2 + y_j^2} \right\} \\
 & - \frac{2(\xi-x_j)^2}{[(\xi-x_j)^2 + y_j^2]^2} - \frac{2(\xi+x_j)^2}{[(\xi+x_j)^2 + y_j^2]^2} \quad (9)
 \end{aligned}$$

$$\beta(y_j, \xi) = \left(\frac{3+\nu}{1+\nu} \right) \left(\frac{1}{\xi^2 + y_j^2} \right) - \left(\frac{2\xi^2}{(\xi^2 + y_j^2)^2} \right) \quad (10)$$

and ξ is the distance from the origin to a loading point on the crack surface. The displacement caused by this stress distribution is obtained from Eq. (1) by using the following complex stress function given by Irwin¹⁶⁾ for the condition with four symmetrical concentrated forces on a crack face as in Fig. 4.

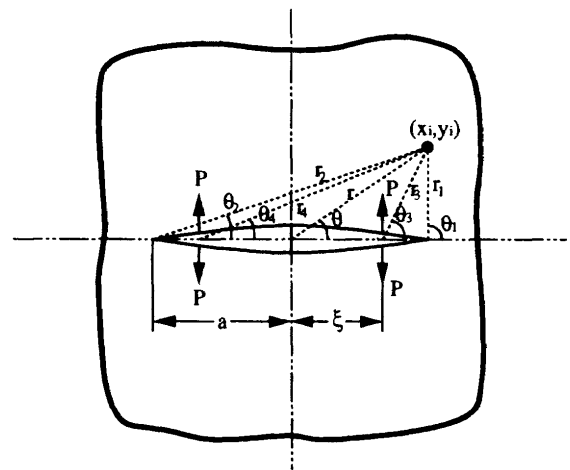


Fig. 4. Concentrated forces applied to the crack face

$$Z = \frac{2Pa}{i\pi(z^2 - \xi^2)} \left| \frac{1 - (\xi/a)^2}{1 - (a/z)^2} \right|^{1/2} \quad (11)$$

By substituting $\sigma_y(x,0) \text{td}\xi$ for P and integrating with respect to ξ over half the crack length, the displacement v_4 is obtained in general as follows

$$v_4 = -\frac{(1+\nu)y_i}{2\pi^2 E t} \left[F_i \int_0^a \alpha(x_i, y_i, \xi) \varepsilon(x_i, y_i, \xi) d\xi + P_j \int_0^a \beta(y_i, \xi) \varepsilon(x_i, y_i, \xi) d\xi \right] \quad (12)$$

where ε is the following

$$\varepsilon(x_i, y_i, \xi) = \log \left[\frac{(a^2 - \xi^2) + (a^2 - \xi^2)^{1/2} (BC + AD) + r_1 r_2}{(a^2 - \xi^2) - (a^2 - \xi^2)^{1/2} (BC + AD) + r_1 r_2} \right] - \frac{y_i (1 + \nu) (a^2 - \xi^2)^{1/2}}{r_1 r_2 r_3^2 r_4^2} \{ [x_i^2 - \xi^2 - y_i^2] [x_i (AC - BD) + y_i (BC + AD)] - 2x_i y_i [x_i (BC + AD) - y_i (AC - BD)] \} \quad (13)$$

where

$$\begin{aligned} A &= (r_1 + x_i - a)^{1/2}, \\ B &= (r_1 - x_i - a)^{1/2}, \\ C &= (r_2 + x_i - a)^{1/2}, \\ D &= (r_2 - x_i - a)^{1/2}, \end{aligned}$$

and r_1, r_2, r_3 , and r_4 are defined in Fig. 4. Eq. (12) is integrated numerically.

Therefore, the total sheet displacement v_T is given as the following:

$$v_T = v_1 + v_2 + v_3 + v_4 \quad (14)$$

2.2.2 Outer Intact Stiffener Displacements

Outer intact stiffener displacement δ_{D_i} from direct fastener loads is given by

$$\delta_{D_i} = (1/A_s E_s) \sum_{j=n+1}^i F_j y_j + (y_j/A_s E_s) \sum_{j=i+1}^{2n} F_j \quad (15)$$

where A_s and E_s are a cross-sectional area and Young's modulus of the stiffener, respectively, and n is the number of fasteners on a stiffener in analysis domain.

Outer intact stiffener displacement δ_{D_i} resulting from gross stress is given by

$$\delta_{G_i} = \sigma y_i / E_s \quad (16)$$

2.2.3 Center Broken Stiffener Displacements

In this case, stiffener displacement δ_{D_i} by direct fastener loads is as follows

$$\delta_{D_i} = (1/A_s E_s) \sum_{j=1}^i P_j (y_n - y_i) + (1/A_s E_s) \sum_{j=i+1}^{n-1} P_j (y_n - y_j) \quad (17)$$

2.2.4 Fastener Displacements

The elastic i -th fastener displacement δ_{F_i} in shear is given by the following empirical relationship¹⁷⁾

$$\delta_{F_i} = (F_{f_i} / Ed) \left[C_1 + C_2 \left(\frac{d}{t} + \frac{d}{t_s} \right) \right] \quad (18)$$

where W, X are applied the i -th fastener load and thickness of stiffener, respectively, and C_1, C_2 are constants determined by Swift's experiments¹⁷⁾. A diagram of fastener displacement is shown in Fig. 5.

2.2.5 Compatibility of Displacements

The DCM is based on displacement compatibility between the cracked sheet and the stiffener plus the fastener. Thus, the stiffener displacement plus the fastener displacement is equal to the sheet displacement. Therefore, the following relationship on the i -th fastener is obtained,

$$v_{T_i} = \delta_{D_i} + \delta_{G_i} + \delta_{F_i} \quad (19)$$

By considering the directions of fastener loads and having a different relationship on the displacement compatibility of each stiffener, there are the following relationships on the i -th fastener point; for the center broken stiffener

$$\begin{aligned} & \sum_{j=n+1}^{2n} \{ v_2(x_n, y_n, x_j, y_j) - v_2(x_i, y_i, x_j, y_j) + v_4(x_n, y_n, x_j, y_j) - v_4(x_i, y_i, x_j, y_j) \} \\ & - \sum_{j=1}^n \{ v_3(x_n, y_n, x_j, y_j) - v_3(x_i, y_i, x_j, y_j) + v_4(x_n, y_n, x_j, y_j) - v_4(x_i, y_i, x_j, y_j) \} \quad (20), \\ & + \delta_{F_n} - \delta_{F_i} - \delta_{D_i} = v_1(x_i, y_i) - v_1(x_n, y_n) \end{aligned}$$

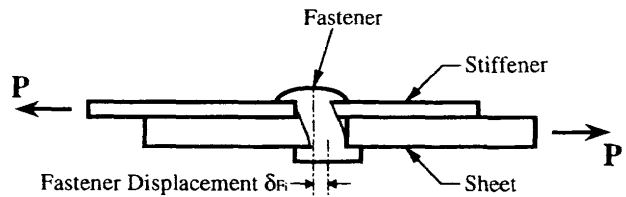


Fig. 5. Schematic diagram of fastener displacement

and for the outer intact stiffener

$$\delta_{F_i} + \delta_{D_i} - \sum_{j=n+1}^{2n} \{v_2(x_i, y_i, x_j, y_j) + v_4(x_i, y_i, x_j, y_j)\} + \sum_{j=1}^n \{v_3(x_i, y_i, y_j) + v_4(x_i, y_i, x_j, y_j)\} = v_1(x_i, y_i) - \delta_{G_i} \quad (21)$$

However, in Eq. (20), the n-th fastener point is selected as a reference point of extension. For the n-th fastener point, that is, $i = n$, though both sides of Eq. (20) equal zero, we can find the following force equilibrium equation

$$\sum_{j=1}^n P_j = \sigma A_s \quad (22)$$

On the right of Eqs. (20) and (21), the displacements are derived from the remote gross stress σ ; on the left of Eqs. (20) and (21), they are derived from the fastener loads P_s and F_s . Therefore, we can make Eqs. (20) and (21) into a matrix form as follows

$$[V] \begin{Bmatrix} P \\ F \end{Bmatrix} = \{V_\sigma\} \quad (23)$$

where V and V_σ are a $2 \times 2n$ matrix and a $2n \times 1$ vector derived numerically from Eqs. (20), (21), and (22), and P, F are unknown fastener loads $n \times 1$ vectors. Thus, solutions of these unknown fastener loads are obtained by inverting the matrix V .

2.2.6 Crack-tip Stress Intensity Factor

Crack-tip stress intensity factor with concentrated forces was derived by Paris¹⁸⁾. Crack-tip stress intensity factors K_{cs} caused by each pair of center stiffener-fastener loads, as shown in Fig. 6 (a), are given by

$$K_{csj} = \left(\frac{P_j \sqrt{a}}{2l \sqrt{\pi}} \right) \left| \frac{2a^2 + (3 + \nu) Y_1^2}{(a^2 + Y_1^2)^{3/2}} \right| \quad (24)$$

and K_{os} caused by each set of outer stiffener-fastener loads, as shown in Fig. 6 (b), are given by

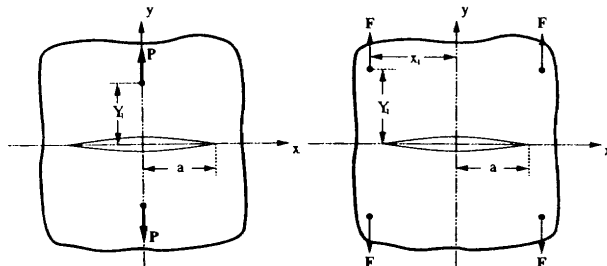


Fig. 6. Schematic diagram of fastener loads in a cracked stiffened panel

$$K_{osj} = \left(\frac{2F_j Y_1 \sqrt{\pi a}}{\pi t} \right) \left| \left(\frac{3 + \nu}{2} \right) I_1 - (1 + \nu) I_2 \right| \quad (25)$$

where

$$I_1 = \gamma / \left| Y_1 \sqrt{(Y_1^2 + a^2 - x_1^2)^2 + 4x_1^2 Y_1^2} \right| \quad (26)$$

$$I_2 = \frac{\left[(a^2 + x_1^2) Y_1 + (a^2 - x_1^2)^2 \right] \gamma^2 + x_1^2 Y_1^2 (Y_1^2 - a^2 + x_1^2)}{2Y_1 \gamma \left[(Y_1^2 + a^2 - x_1^2)^2 + 4x_1^2 Y_1^2 \right]^{3/2}} \quad (27)$$

$$\gamma = \frac{1}{\sqrt{2}} \left| \left[(Y_1^2 + a^2 - x_1^2)^2 + \sqrt{(Y_1^2 + a^2 - x_1^2)^2 + 4x_1^2 Y_1^2} \right]^{1/2} \right| \quad (28)$$

and x_1, Y_1 are horizontal and vertical distance from crack center to fastener load, respectively. Therefore, gross crack-tip stress intensity factor K_{GP} in the cracked stiffened panel is derived by considering the directions of fastener loads as follows

$$K_{GP} = \sigma \sqrt{\pi a} + \sum_{j=1}^n K_{csj} - \sum_{j=n+1}^{2n} K_{osj} \quad (29)$$

where $\sigma \sqrt{\pi a}$ is a crack-tip stress intensity factor of cracked unstiffened sheet. In the DCM, if a half crack length a is given, K_{GP} is calculated, and residual strength analysis of a cracked stiffened panel is given by using K_{GP} .

2.3 Description of a Method of Considering Stochastic Factors

In a residual strength analysis of a cracked stiffened panel, there are many uncertainties regarded as stochastic factors. In this paper, however, only fastener flexibility is considered as a stochastic factor.

From Eq. (18), a fastener displacement δ_{F_i} has a linear relationship to a fastener load F_{F_i} . Thus, Eq. (20) can be written in the form

$$\delta_{F_i} = C_f \times F_{F_i} \quad (30)$$

where

$$C_f = (1/Ed) \left[C_1 + C_2 \left(\frac{d}{T} + \frac{d}{t_s} \right) \right] \quad (31)$$

In Eq. (31), C_1 and C_2 are empirical constants. Therefore, fastener flexibility constant C_f is determined empirically. In practice, however, fastening conditions are not deterministic because they are influenced by some uncertain factors such as fastening force magnitude, fastener hole defects, and fastening relaxation, etc. Thus, C_f represents a mean value of experimental data, that is to say, we can consider that C_f is a random variable in

accordance with a probabilistic distribution. Because so many experiments are needed to make sure of its distribution, it is very difficult to find the distribution. Accordingly, we assumed that the distribution is a normal distribution. In this paper, many data of C_f in accordance with a normal distribution are generating by the Monte Carlo method. Then the distribution of K_{GP} is given by assembling calculations with each C_f data. Effects of stochastic factors to residual strength are shown by investigating results from it.

3. A Study of Differences in Distribution Models of Fastener Flexibility¹⁹⁾

3.1 Description of Models

Now, in order to choose the distribution model of fastener flexibility, three models are investigated here. They are as follows:

Model 1: Every fastener has the same C_f value in the same case and C_f values make up one normal distribution.

Model 2: Every fastener has different C_f values from each other in the same and different cases the total C_f values make up one normal distribution.

Model 3: Only the closest fastener on the center broken stiffener to the crack has a C_f value in accordance with one normal distribution but the other fasteners have a determined C_f value.

Model 1 is a simulation of the case in which the C_f value itself is uncertain, Model 2 is a simulation of the case in which the fastening system is uncertain, and Model 3 is proposed to investigate the contribution of only the most effective fastener.

3.2 Details of the Panel Model

The cracked stiffened panel is assumed to be the same panel as in reference 6 except for the different section geometry of the stiffeners, which are strip stiffeners in this paper and are hat section stiffeners in reference 6. The material of the panel is 2024 T3 and that of the extended stiffeners is 7075 T6. The fasteners are NAS 1097 DD6 rivets. So the cracked stiffened panel model has the following data; $b = 0.2032$ m, $p = 0.03175$ m, $d = 0.0047625$ m, $E = 7.17 \times 10^{10}$ MPa, $t = 0.0018$ m, $n = 0.3$, $E_s = 7.10 \times 10^{10}$ MPa, $t_s = 0.0018$ m, $A_s = 0.000353$ m², $C_1 = 5.0$, and $C_2 = 0.8$ where b is a stiffener spacing and p is a fastener spacing. The number of considered fastener points is 15 because, according to reference 6, no advantage can be gained by increasing this problem size beyond 15 fasteners on each side of the crack in each stiffener. Therefore, n is 15 in Eqs. (15), (17), (20)-(22) and (29), and the size of the matrix in Eq. (23) is 30×30 .

3.3 Results and Discussion

Data for y are generated by the Monte Carlo method under the normal distribution, the mean value of which is the determined z value and standard deviations of which are 10 % or 20 % of the determined C_f value. In practice, data for C_f are given by the following relation:

$$C_f = C_{f0} (1 + \alpha_s \cdot \alpha_f) \tag{32}$$

where C_{f0} is the determined C_f value which is given by Eq. (31), α_f is a value of the standard normal distribution which is given by the Box-Muller method²⁰⁾, and α_s is a weight coefficient. That is, if the data for C_f have a standard deviation of 10 %, α_s is 0.1 because, ideally, for the distribution of α_f , the mean value is 0 and the standard deviation is 1. For Model 1 and Model 3, the number of data for C_f is 1000. For the distribution of α_f , therefore, the mean value is -0.057596 and the standard deviation is 0.97962. While for Model 2, because the number of fasteners is 30, the number of data for C_f is 30000. For the distribution of α_f , therefore, the mean value is -0.0071218 and the standard deviation is 0.99994.

The results of each model are shown in Tables 1-4. Where in the tables, a/b is obtained by dividing a half crack length by the stiffener spacing, β_0 is obtained by dividing K_{GP} , gross crack-tip stress intensity factor in the cracked stiffened panel, by $\sigma\sqrt{\pi a}$, which is a crack-tip stress intensity factor of cracked unstiffened sheet, with using the deterministic C_f value from Eq. (32), $\mu\{\beta_0\}$, $s\{\beta_0\}$ are a mean value and a standard deviation, respectively. M1-10 % means Model 1 in the case of 10 % standard deviation of C_f , and so on, $\Delta\beta_0$ (0.9!) means the deviation between β_0 and

Table 1. Results from Model 1 in the case of 10% standard deviation of C_f

a/b	β_0	$\mu\{\beta_0\}$: M1-10 %	$s\{\beta_0\}$: M1-10 %	$\Delta\beta_0$ (0.9 C_f)	$\Delta\beta_0$ (1.1 C_f)
0.0625	2.5187	2.5219 (+ 0.0032)	0.030332 (1.20 %)	+ 0.032	- 0.0291
0.25	1.6544	1.6548 (+ 0.0004)	0.0040152 (0.24 %)	+ 0.0042	- 0.0039
0.50	1.3651	1.3650 (+ 0.0001)	0.00031292 (0.02 %)	+ 0.0004	- 0.0003
0.75	1.1968	1.1965 (+ 0.0003)	0.0022586 (0.19 %)	+ 0.0024	- 0.0022
1.0	0.88411	0.88284 (- 0.00127)	0.012189 (1.38 %)	- 0.01286	+ 0.0117
1.25	0.64350	0.64280 (- 0.0007)	0.015050 (2.34 %)	- 0.01579	+ 0.01466

Table 2. Results from Model 1 in the case of 20% standard deviation of C_f

a/b	β	$\mu[\beta]: M1-20\%$	$s[\beta]: M1-20\%$	$\Delta\beta: (0.8 C_f)$	$\Delta\beta: (1.2 C_f)$
0.0625	2.5187	2.5283 (+ 0.0096)	0.063005 (2.49 %)	+ 0.0677	- 0.0555
0.25	1.6544	1.6555 (+ 0.0011)	0.0081918 (0.49 %)	+ 0.0088	- 0.0075
0.50	1.3651	1.3650 (+ 0.0001)	0.00062593 (0.05 %)	+ 0.0007	- 0.0006
0.75	1.1968	1.1962 (+ 0.0006)	0.0045769 (0.38 %)	+ 0.0049	- 0.0043
1.0	0.88411	0.88033 (- 0.00378)	0.025310 (2.88 %)	- 0.0271	+ 0.0224
1.25	0.64350	0.63950 (- 0.004)	0.030812 (4.82 %)	- 0.03286	+ 0.02834

Table 3. Results from Model 2 and 3 in the case of 10% standard deviation of C_f

a/b	β	$\mu[\beta]: M2-10\%$	$s[\beta]: M2-10\%$	$\mu[\beta]: M3-10\%$	$s[\beta]: M3-10\%$
0.0625	2.5187	2.5204 (+ 0.0017)	0.037787 (1.50 %)	2.5231 (+ 0.0044)	0.037547 (1.49 %)
0.25	1.6544	1.6548 (+ 0.0002)	0.0047575 (0.29 %)	1.6548 (+ 0.0004)	0.0031157 (0.19 %)
0.50	1.3651	1.3650 (+ 0.0001)	0.0013372 (0.10 %)	1.3651 (± 0.0)	0.000489 (0.04 %)
0.75	1.1968	1.1966 (+ 0.0002)	0.0010132 (0.08 %)	1.1968 (± 0.0)	0.000134 (0.01 %)
1.0	0.88411	0.88322 (- 0.00089)	0.0067228 (0.76 %)	0.88412 (+ 0.00001)	0.0000363 (0.004 %)
1.25	0.64350	0.64249 (- 0.00101)	0.0083406 (1.30 %)	0.64350 (+ 0.0)	0.0000036 (0.0005 %)

Table 4. Results from Model 2 and 3 in the case of 20% standard deviation of C_f

a/b	β	$\mu[\beta]: M2-10\%$	$s[\beta]: M2-10\%$	$\mu[\beta]: M3-10\%$	$s[\beta]: M3-10\%$
0.0625	2.5187	2.5256 (+ 0.0069)	0.078593 (3.11 %)	2.5325 (+ 0.0138)	0.079211 (3.13 %)
0.25	1.6544	1.6553 (+ 0.0009)	0.0098529 (0.60 %)	1.6555 (+ 0.0011)	0.0065376 (0.39 %)
0.50	1.3651	1.3649 (+ 0.0002)	0.0027735 (0.20 %)	1.3652 (+ 0.0001)	0.0010260 (0.08 %)
0.75	1.1968	1.1960 (+ 0.0008)	0.0021247 (0.18 %)	1.1968 (± 0.0)	0.00028130 (0.02 %)
1.0	0.88411	0.88041 (- 0.0037)	0.014306 (1.62 %)	0.88413 (+ 0.0002)	0.0000762 (0.009 %)
1.25	0.64350	0.63931 (- 0.00419)	0.017449 (2.73 %)	0.64350 (± 0.0)	0.0000757 (0.01 %)

one which is obtained by substituting $0.9 C_f$ for C_f the other $\Delta\beta_0$ s mean in the same way, and % values are obtained by dividing $s[\beta_0]$ by $\mu[\beta_0]$ on each a/b.

Common results in three models are as follows: every $\mu[\beta_0]$ has a slight deviation to β_0 on each a/b and $s[\beta_0]$ in the case of 20 % standard deviation are not twice as much as that of 10 %; that is, the relationship between $s[\beta_0]$ and the assumed standard deviation of C_f is not linear. Results from each model are as follows: for Model 1, results from a constant C_f changed simply by 10 % in magnitude are different from those assuming a 10 % standard deviation, and stochastic factors in fastener flexibility affect the crack-tip stress intensity factor when the crack length is very short or close to a two-bay crack and longer; for Model 2, stochastic factors affect the crack-tip stress intensity factor the same as in Model 1; and for Model 3, stochastic factors in fastener flexibility affect the crack-tip stress intensity factor only when the crack length is very short.

We infer from these results that, in the case of a very short crack, stochastic factors in the first fastener on the center broken stiffener dominate the results, and in the case of close to a two-bay crack and more, Model 1 affects the results easier than Model 2 because all fasteners have the same C_f in Model 1 and every fastener has a different C_f in Model 2. Therefore, the deviation of C_f in Model 1 is more effective than that in Model 2.

4. Results and Discussion of Residual Strength Analysis²¹⁾

In this paper, the residual strength of a cracked stiffened panel is defined as the stress where the residual strength of the sheet is equal to the outer stiffener strength criterion because, in the event that the former is higher than the latter, a fast fracture could not be arrested by the outer stiffeners.

The residual strength of the sheet σ_R and the outer stiffener strength criterion F_{ssc} are shown to have the following relationships

$$\sigma_R = \frac{K_{GP}}{\beta_0 \sqrt{\pi a}} = \frac{\sigma K_C}{K_{GP}} \quad (33)$$

where $!Q$ is obtained from Eq. (29), K_c , fracture toughness of the sheet material, which is 2024 T3, is $211.4 \text{ MN/m}^{3/2}$ and

$$\beta_0 = \frac{K_{GP}}{\sigma \sqrt{\pi a}} \quad (34)$$

and

$$F_{ssc} = F_{US} \frac{\sigma}{\sigma_s} \quad (35)$$

where $F_{U_{ST}}$, the ultimate strength of the outer stiffener material, which is 7075 T6, is 583.3 MN/m^2 and σ_s is the outer stiffener stress.

From section 3.3, Model 1 has the most effective results of the three models. Model 2, however, represents the best practical case because it is difficult to consider all fasteners as having the same C_f as in Model 1, and only one fastener has the uncertainties like Model 3, and it is reasonable to consider of every fastener as having various fastener flexibility. Therefore, in the residual strength analysis, Model 2 is adopted as the model of stochastic factors in fastener flexibility. Regarding the panel model, the same model as in section 3 is used here. In this analysis, data for C_f are generated by the Monte Carlo method, as in Model 2 in section 3.3.

The results of analysis are shown in Figs. 7 and 8 as the relation of a/b to strength (MPa) at about 10 % and 20 % standard deviation for C_f , respectively. In these figures, the ERSS line is the calculated expectation line of the residual strength of the sheet σ_R , obtained from Eq. (33), and the ESSC line is that of the outer intact stiffener strength criterion E_{SSC} , obtained from Eq. (35). +3s means the expectation value plus three times the calculated standard deviation, and -3s means the same as +3s except minus three times the calculated standard deviation. That is, the probability that σ_R and E_{SSC} are in the region from -3s line to +3s line is 99.7 % in each case. In an analysis by deterministic values; that is, using the ERSS and ESSC lines; in the region $a/b < 1.2$, if the strength is under Point B, the panel never fractures. However, if the strength is beyond Point B, the sheet

will fracture. For example, if a/b equals 0.5 and the strength is at Point A, a fast fracture will occur and stop at Point C. Then increasing stress to Point E, at that point the outer intact stiffener will break and the strength of the panel will fall rapidly and the panel will fracture. Therefore, in the deterministic analysis, Point E shows the residual strength point and the residual strength is 344MPa. On the other hand, in this analysis, the residual strength has an interval from Point D to Point F in each case. The probability that the residual strength is in the interval is 99.7 %, and the intervals are from 336MPa to 353MPa in the case of Fig. 7 and from 324MPa to 360MPa in the case of Fig. 8. Thus, the ratios of those intervals to the deterministic residual strength are 4.9 % for Fig. 7 and 10.5 % for Fig. 8. We infer from these results that stochastic factors in fastener flexibility affect the residual strength of the panel considerably and can not be ignored because the residual strength is one of the standards of a panel design in damage tolerance design.

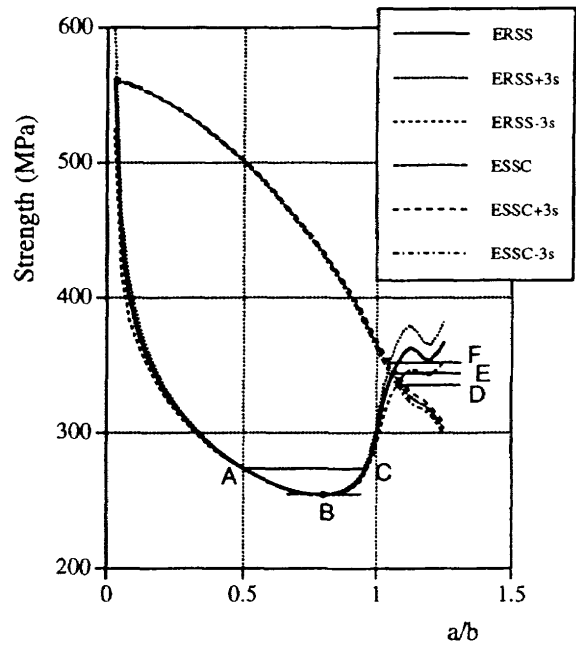


Fig. 7. Residual strength diagram in the case of 10 % standard deviation for C_f

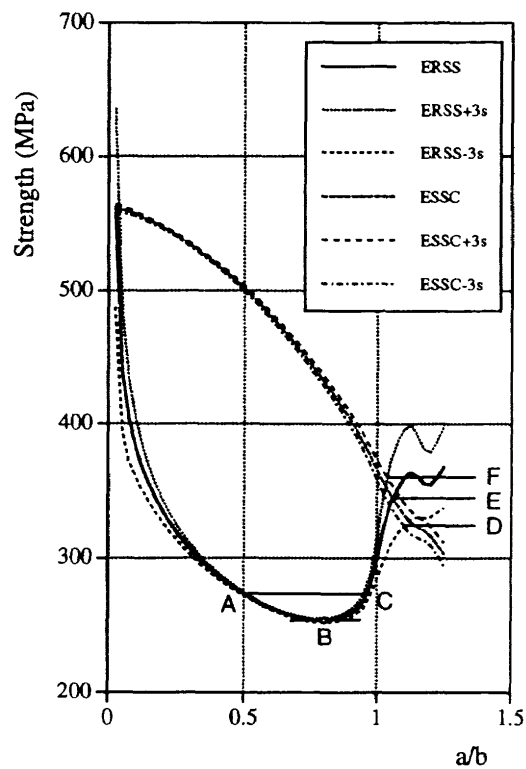


Fig. 8. Residual strength diagram in the case of 20 % standard deviation for C_f

5. Conclusions

The differences in stochastic distribution models for fastener flexibility are shown. It is shown that stochastic factors in fastener flexibility affect the residual strength of the cracked stiffened panel considerably and can not be ignored in designing

stiffened panels in damage tolerance design. Hereafter, in order to be more practical, this work ought to be continued with many considerations; for example, the effects of stiffener bending, non-linearity in fastener flexibility, fastener failure criterion, reliability analysis, and other stochastic factors should be included.

Acknowledgements

The author wishes to thank Mr. Tom Swift, National Resource Specialist in Federal Aviation Administration, for his valuable advices on the displacement compatibility method, and Dr. Hiroo Asada, Head of Engineering Section in Airframe Division in NAL, for providing the opportunity to carry out this work.

Reference

- 1) Docket No.27358; Notice No.93-9, Federal Register, Vol.58, No.136, July 19, 1993, Proposed Rules, pp.38642-38646.
- 2) Swift, T.; Damage Tolerance Capability, Fatigue, Vol.16, No.1, 1994, pp.75-94.
- 3) Damage Tolerance Assessment Handbook Volume I: Introduction, DOT/FAA/CT-93/69.1, October, 1993.
- 4) Poe, C.C., Jr.; Stress-Intensity Factor for a Cracked Sheet with Riveted and Uniformly Spaced Stringers, NASA TR R-358, May, 1971.
- 5) Poe, C.C., Jr.; The effect of Broken Stringers on the Stress Intensity Factor for a Uniformly Stiffened Sheet Containing a Crack, NASA TM X-71947, 1974.
- 6) Swift, T.; The Effects of Fastener Flexibility and Stiffener Geometry on the Stress Intensity in Stiffened Cracked Sheet, Proceedings of an International Conference on 'Prospects of Fracture Mechanics,' Held at Delft University of Technology, the Netherlands, June 24-28, 1974, pp.419-436.
- 7) Swift, T.; Fracture Analysis of Stiffened Structure, Damage-Tolerance of Metallic Structures: Analysis Methods and Application, ASTM STP842, 1984, pp.69-107.
- 8) JADC-KHI:KR-14315, 1984 (in Japanese).
- 9) JADC-KHI:KR-14451, 1985 (in Japanese).
- 10) Nishimura, T.; Stress Intensity Factors for a Cracked Stiffened Sheet with Cracked Stiffeners, Journal of Engineering Materials and Technology, Transactions of the ASME, Vol.113, January, 1991, pp.119-124.
- 11) Nishimura, T.; Stress Intensity Factors of Multiple Cracked Sheet with Riveted Stiffeners, Journal of Engineering Materials and Technology, Transactions of the ASME, Vol.113, July, 1991, pp.280-284.
- 12) Nishimura, T.; Strip Yield Analysis for Multiple Cracked Sheet with Riveted Stiffeners, Journal of Engineering Materials and Technology, Transactions of the ASME, Vol.115, October, 1993, pp.398-403.
- 13) Yeh, J.R.; Fracture Analysis of a Stiffened Orthotropic Sheet, Engineering Fracture Mechanics, Vol.46, No.5, 1993, pp.857-866.
- 14) Westergaard, H.M.; Bearing Pressures and Cracks, Journal of Applied Mechanics, Transactions of the ASME, Vol.6, No.2, June, 1939, pp. A-49-A-53.
- 15) Love, A.E. H.; A Treatise on the Mathematical Theory of Elasticity, Fourth ed. (First American Printing), Dover Publ., 1944, p.209.
- 16) Irwin, G.R.; Analysis of Stresses and Strains Near the End of a Crack Traversing a Plate, Journal of Applied Mechanics, Transactions of the ASME, Vol.24, 1957, pp.361-364.
- 17) Swift, T.; Development of the Fail-Safe Design Features of the DC-10, Damage Tolerance in Aircraft Structures, ASTM STP 486, 1971, pp.164-214.
- 18) Paris, P.C.; Application of Muskhelishvili's Method to the Analysis of Crack Tip Stress Intensity Factors for Plane Problems, Part III. Inst. Research, Lehigh University, June, 1960.
- 19) Shoji, H.; A Residual Strength Analysis for a Cracked Stiffened Panel with Consideration of Stochastic Factors in Rivet Fastening (2nd Report), Proceedings of the 37th Meeting on the JSASS/JSME Structures Conference, July, 1995, pp.113-116 (in Japanese).
- 20) Watanabe, T., Natori, R. and Oguni, T.; Numerical Calculation SOFTWARE with FORTRAN77, Maruzen, December, 1989, pp.321-322 (in Japanese).
- 21) Shoji, H.; A Residual Strength Analysis of a Stiffened Panel with Considering Uncertainties, National Aerospace Laboratory News, No.437, September, 1995, pp.7-8 (in Japanese).

航空宇宙技術研究所報告1283T号

平成8年2月発行

発行所 航空宇宙技術研究所
東京都調布市深大寺東町7丁目44番地1
電話三鷹(0422)47-5911(大代表)〒182
印刷所 株式会社 東京プレス
東京都板橋区桜川2-27-12

Printed in Japan